

## Coexistence of ferromagnetism and superconductivity in $\text{ErRh}_4\text{B}_4$ single crystals probed by dynamic magnetic susceptibility

R. Prozorov,\* M. D. Vannette, S. A. Law, S. L. Bud'ko, and P. C. Canfield

*Ames Laboratory and Department of Physics and Astronomy, Iowa State University, Ames, Iowa 50011, USA*

(Received 26 January 2008; published 7 March 2008)

High-resolution measurements of the dynamic magnetic susceptibility are reported for the ferromagnetic, reentrant superconductor  $\text{ErRh}_4\text{B}_4$ . A detailed investigation of the coexisting regime reveals unusual temperature-asymmetry on warming and cooling and magnetically anisotropic behavior. The superconducting phase appears via a series of discontinuous steps upon warming from the ferromagnetic normal phase, whereas the ferromagnetic phase develops via a more gradual transition upon cooling from the superconducting phase. A model based on local field inhomogeneity is proposed to explain these observations.

DOI: [10.1103/PhysRevB.77.100503](https://doi.org/10.1103/PhysRevB.77.100503)

PACS number(s): 74.25.Dw, 74.25.Ha, 75.50.Cc

Problems associated with the coexistence of long-range magnetic order and superconductivity were discussed even before the appearance of the microscopic theory of superconductivity.<sup>1</sup> This topic remains one of the most interesting and controversial in the physics of superconductors, with many reviews and books devoted to the subject.<sup>2-6</sup> Despite significant effort in new materials design and discovery, there are only a few confirmed ferromagnetic (FM) superconductors (SC). Local, full-moment ferromagnetic superconductors  $\text{ErRh}_4\text{B}_4$  ( $T_{\text{FM}} \approx 0.9$  K,  $T_c \approx 8.7$  K),<sup>7</sup>  $\text{Ho}_x\text{Mo}_6\text{S}_8$  ( $T_{\text{FM}} \approx 0.7$  K,  $T_c \approx 1.8$  K),<sup>8</sup> the weakly ferromagnetic  $\text{ErNi}_2\text{B}_2\text{C}$  ( $T_{\text{FM}} \approx 2.3$  K,  $T_{\text{AFM}} \approx 6$  K,  $T_c \approx 11$  K),<sup>9</sup> and more recent itinerant superconducting ferromagnets  $\text{UGe}_2$  ( $T_{\text{FM}} \approx 33$  K,  $T_c \approx 0.95$  K) at  $P \approx 1.3$  GPa (Ref. 10) and  $\text{URhGe}$  ( $T_{\text{FM}} \approx 9.5$  K,  $T_c \approx 0.27$  K).<sup>11</sup> Whereas all these materials are very interesting on their own, the coexistence of growing, large, local moment ferromagnetism and superconductivity is most clearly presented in  $\text{ErRh}_4\text{B}_4$ . In particular, we are interested in the details of the narrow temperature interval ( $\sim 0.3$  K) where the two phases coexist and influence each other.

$\text{ErRh}_4\text{B}_4$  has been extensively studied over the past 30 years.<sup>2-6,12,13</sup> The ferromagnetic phase is primitive tetragonal where the  $c$  axis is the hard axis and the  $a$  axis is the easy magnetic axis. Detailed measurements of anisotropic magnetization upper  $H_{c2}$  and lower  $H_{c1}$  critical fields were done by Crabtree *et al.*<sup>13,14</sup> who found that  $H_{c2}^a$  (along the  $a$  axis) peaks at 5.5 K due to large paramagnetic spin susceptibility in that direction and then merges with  $H_{c1}$  at low temperature indicating a transition to type-I superconducting state.<sup>13,4</sup> In contrast,  $H_{c2}^c$  collapses near the onset of the long-range ferromagnetic order.

Neutron-diffraction studies have established the existence of a modulated ferromagnetic structure with a length scale of  $\sim 10$  nm.<sup>15,16</sup> Single-crystal data suggested that coexisting phases form a mosaic of normal FM domains and SC regions larger than  $\sim 200$  nm in size. The SC regions contain modulated FM moment with a period of  $\sim 10$  nm. These regions could be regular domains, spontaneous vortex lattices, or laminar structures with  $\geq 200$  nm periodicity and modulated SC domains in between.<sup>16</sup> Thermal hysteresis is observed both in the normal Bragg peak intensity and the small-angle peaks. For the small-angle peaks, the intensity is higher on

cooling than on warming. This is opposite to the behavior of the regular Bragg peaks from the FM regions.<sup>15</sup> Furthermore, the first-order transition, observed in satellite peaks' temperature dependence,<sup>16</sup> is consistent with the spiral state of Blount and Varma.<sup>17</sup> However, a continuous transition was reported in other neutron diffraction studies<sup>15,18</sup> and specific heat experiments.<sup>19</sup> Such a transition can be realized in a modulated structure or via the formation of a spontaneous vortex phase.

Theoretically, some striking features of the coexisting phase include an inhomogeneous spiral FM structure,<sup>17,20</sup> a fine domain "cryptoferromagnetic" phase,<sup>2,21</sup> a vortex-lattice modulated spin structure,<sup>22</sup> type-I superconductivity,<sup>2,22,23</sup> a gapless regime, and, possibly, an inhomogeneous Fulde-Ferrell-Larkin-Ovchinnikov (FFLO) state.<sup>2,12</sup> Another interesting possibility is the development of superconductivity at the ferromagnetic domain walls.<sup>24,25</sup>

In this paper we report precision measurements of the dynamic magnetic susceptibility of  $\text{ErRh}_4\text{B}_4$  with an emphasis on the narrow temperature region where ferromagnetism and superconductivity coexist. We find that the transition is hysteretic and also highly asymmetric when  $\text{FM} \rightarrow \text{SC}$  (heating) and  $\text{SC} \rightarrow \text{FM}$  (cooling) data are compared. The  $\text{FM} \leftrightarrow \text{SC}$  transition proceeds via a series of discrete steps from the FM to the SC phase upon warming and proceeds via a smooth crossover from the SC to the FM state upon cooling. With this new information we analyze the relevance of some of the predictions made over the years for the coexisting phase.

Single crystals of  $\text{ErRh}_4\text{B}_4$  were grown at high temperatures from a molten copper flux as described in Refs. 26 and 27. The resulting samples were needle shaped with the crystallographic  $c$  axis along the needles. Transport measurements gave a residual resistivity ratio (RRR) of about 8, consistent with previous reports. (Note that significant contribution to resistivity comes from spin-disorder scattering, so this low value of RRR does not indicate bad sample quality.) The anisotropic  $H_{c2}(T)$  curves (see inset to Fig. 4 below) are consistent with earlier reports as well.<sup>13,14</sup>

The ac magnetic susceptibility  $\chi$  was measured with a tunnel-diode resonator (TDR) which is sensitive to changes in susceptibility  $\Delta\chi \sim 10^{-8}$ . Details of the measurement technique are described elsewhere.<sup>28-30</sup> In brief, a properly bi-

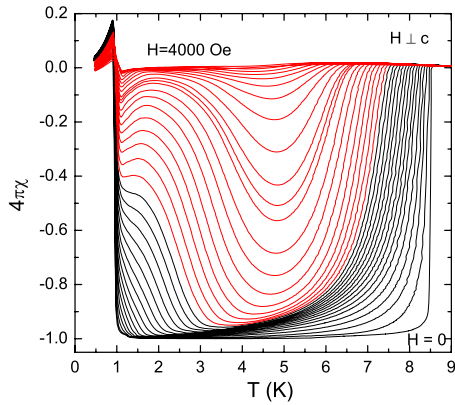


FIG. 1. (Color online) The dynamic magnetic susceptibility of a  $\text{ErRh}_4\text{B}_4$  single crystal measured along the magnetic easy axis (perpendicular to the needle-shaped sample). Each curve corresponds to a fixed value of the applied dc magnetic field in the range indicated in the figure. The red curves (gray in print) correspond to measurements where  $4\pi\chi(T)$  becomes nonmonotonic in the vicinity of the FM-SC transition.

ased tunnel diode compensates for losses in the tank circuit, so it is self-resonating at its resonant frequency,  $\omega = 1/\sqrt{LC} \sim 10$  MHz. A sample is inserted into the coil on a sapphire rod. The effective inductance changes and this causes a change in the resonant frequency. This frequency shift is the measured quantity and it is proportional to the sample's dynamic magnetic susceptibility  $\chi$ .<sup>28–30</sup> Knowing the geometrical calibration factors of our circuit, we obtain  $\chi(T, H)$ . The advantages of this technique are: very small ac excitation field amplitude ( $\sim 20$  mOe), which means that it only probes but does not disturb the superconducting state; high stability and excellent temperature resolution ( $\sim 1$  mK), allowing a detailed study of the coexisting region, which is only  $\sim 500$  mK wide. The normal-state skin depth is larger than the sample size, so we probe the entire bulk, but when the superconducting phase becomes dominant, there is the possibility that some FM patches still exist, but are screened.

Figure 1 shows the magnetic susceptibility  $\chi$  in single-crystal  $\text{ErRh}_4\text{B}_4$  for an applied field oriented along the easy axis and perpendicular to the needle-shaped crystal over a wide temperature range. The peak in  $\chi(T)$  at the ferromagnetic to superconducting boundary below 1 K is a common feature observed in local moment ferromagnets.<sup>31</sup> Clearly, superconductivity is fully suppressed in the ferromagnetic phase. Note that at elevated fields, the response is nonmonotonic on the SC side close to the FM boundary, indicative of enhanced diamagnetism (larger, negative  $\chi$ ), which may be due to suppressed magnetic pair breaking or entering into another phase, such as FFLO.<sup>2,12</sup>

Figure 2 zooms into the SC  $\leftrightarrow$  FM transition region. Measurements were taken after zero-field cooling, applying external field and warming up (ZFC-W) to above  $T_c$  and then cooling back to the lowest temperature (FC-C). There is a striking asymmetry in this transition—when the superconducting phase develops out of the FM state, the response proceeds with jumps in the susceptibility, which are clearly associated with the appearance of superconducting regions of

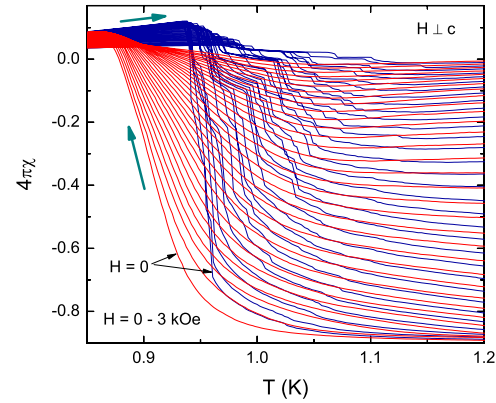


FIG. 2. (Color online) The dynamic magnetic susceptibility of the ferromagnet-superconductor transition in  $\text{ErRh}_4\text{B}_4$  measured at different applied fields. Note the temperature scale and highly asymmetric character of the FM-SC and SC-FM transitions. Blue (dark gray): warming, red (lighter gray): cooling.

finite size. The steps are present up to the largest field in which superconductivity survives. Decreasing temperature results in a completely different behavior: the transition is smooth and gradual as the sample cools.

To better understand the dynamics of the transition, the top frame of Fig. 3 shows measurements at  $H=0$  for different temperature ramp rates that vary over two orders of magnitude. Temperature variation is shown in the inset. These data clearly demonstrate that this hysteresis is insensitive to heating and cooling rates. It should be noted that all the other data presented in this paper were taken with the slowest cooling rate of  $60 \mu\text{K/s}$ .

A similar hysteresis is also present when the external magnetic field is applied along the  $c$  axis. This is shown in Fig. 4. Note that the peak in  $\chi(T)$  at the FM boundary is not present, which is consistent with the behavior observed in other anisotropic, local-moment ferromagnets.<sup>31</sup> The inset to

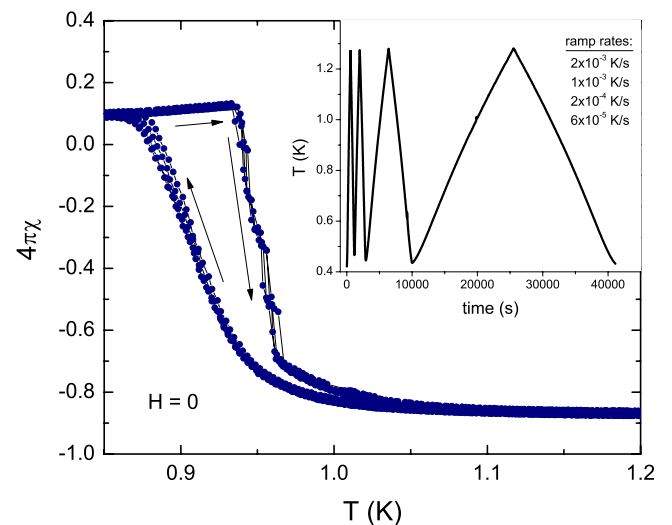


FIG. 3. (Color online) Hysteresis of the transition in zero applied field, measured at different ramp rates. The temperature sweep profiles are shown in the inset.

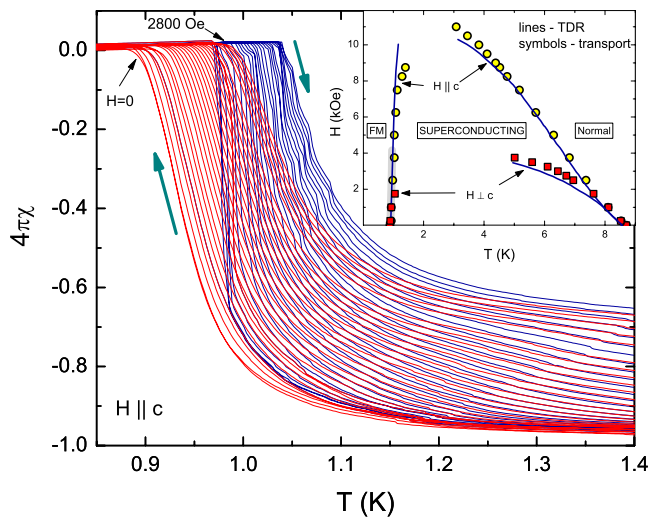


FIG. 4. (Color online) Transition region measured for magnetic field oriented along the needle and  $c$  axis. Inset: summary phase diagram for two orientations measured by transport (symbols) and TDR.

Fig. 4 shows the phase diagram obtained from resistivity and TDR measurements for both orientations. There is excellent agreement between the two techniques and, as noted earlier, this diagram is consistent with previous reports.<sup>13,14</sup>

Finally, Fig. 5 shows so-called minor hysteresis loops (not as a function of field but temperature). The labels show the evolution of the susceptibility. The temperature sweep starts from low temperature at (1) when the sample was then warmed up past the first signs of superconductivity that appear as a small jump at (2) and warmed further, reaching almost full superconductivity at (3). The sample was then cooled back down to (4) as indicated by the arrow and warmed back to (5). Note that along (3)→(4),  $\chi$  is significantly different from (4)→(5). Another similar minor

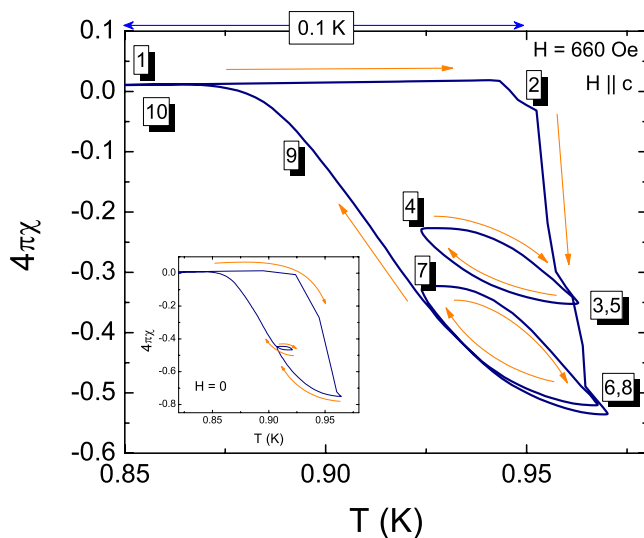


FIG. 5. (Color online) Details of the hysteresis with partial scans as explained in the text. The inset shows another partial loop on a cooling part of the curve.

cooling-warming loop was performed, (6)→(7)→(8), after which the sample was cooled down to return to (10)=(1) via (9). Interestingly, no steps or jumps were observed on the minor loops even on warming. Also, the slope  $d\chi/dT$  is similar on cooling and warming and is very different from the original steep slope (2)→(3). This is consistent with the presence of vortices, probably pinned by the modulated FM/SC structure. The inset in Fig. 5 shows a small minor loop on a cooling part. This loop has small slope comparable to the larger loops described in the main frame.

Let us now turn to the interpretation of these results. Clearly, the FM→SC transition proceeds via a series of jumps in diamagnetic screening due to formation of superconducting regions of macroscopic volume, roughly 5–20 % of the sample volume depending on the applied field and temperature. Indeed, each observed step may be the result of the simultaneous formation of many individual superconducting domains of similar size. These steps in  $\chi$  are present both for  $H||c$  and  $H||a$ , although in the latter case the steps are smaller and more pronounced, possibly due to magnetic and shape anisotropies. The number of steps increases with the increasing field and the first step (the first sign of superconductivity) occurs at a higher temperature for larger applied field. Overall, the FM→SC transition is apparently first order and, as discussed below, is probably a transition to a type-I superconducting state such as that proposed in Refs. 2, 13, 22, and 23.

In our interpretation, the first jump occurs at a temperature where the internal field becomes equal to a “supercooling” field of a type-I superconductor. (Note that during the FM→SC transition we progress deeper into the superconducting phase on warming. This would correspond to a cooling of a regular type-I superconductor.<sup>19,32</sup>) When the first superconducting domains appear, the effective magnetic field in normal regions around them increases due to the flux expulsion. This net increase in the internal field in the remaining FM regions stabilizes them to higher temperatures. The system now needs to go to a higher temperature, deeper into the SC state to produce more superconducting phase. In this scenario, the observed jumps in  $\chi$  correspond to a cascade of such “supercooling” transitions. If the temperature is lowered before the transition is complete, the domains remain stable to lower temperatures, due to physics similar to “superheating” of a type-I superconductor. It is also quite possible that the superconducting domains have the modulated spin structure seen in neutron scattering.<sup>16</sup> Finally, it seems that the number of ferromagnetic domains or their boundaries are not directly related to the observed steps, because at higher fields, the number of these domains decrease and dominant domains (along the applied field) grow in size.

In striking contrast with the FM→SC transition, the SC→FM transition is smooth and proceeds to lower temperatures. Recent works show that in type-I superconductors an intermediate state is highly asymmetric with respect to the increase or decrease of the magnetic field.<sup>33</sup> Therefore it is quite possible that flux tubes are being generated when the system crosses smoothly into the normal, FM phase. It is also possible that a ferromagnetic modulation with a period of  $\sim 10$  nm develops and this would be compatible with the

long-range coherence observed in neutron scattering experiments.<sup>16</sup> We note that the unusual, nonmonotonic behavior of  $\chi$  in the vicinity of the FM boundary from the SC side, could be due to an FFLO state suggested by Bulaevskii for  $\text{ErRh}_4\text{B}_4$ .<sup>2</sup> If we plot the temperature of the minimum in  $\chi(T)$  as a function of applied field, we obtain a phase diagram remarkably similar to Fig. 7 of Ref. 2.

Discussions with Lev Bulaevskii, Alexander Buzdin, Vladimir Kogan, Kazushige Machida, and Roman Mints are appreciated. The work at Ames Laboratory was supported by the Department of Energy-Basic Energy Sciences under Contract No. DE-AC02-07CH11358. R.P. acknowledges support from NSF Grant No. DMR-05-53285 and the Alfred P. Sloan Foundation.

\*prozorov@ameslab.gov

- <sup>1</sup>V. L. Ginzburg, *Sov. Phys. JETP* **4**, 153 (1957).
- <sup>2</sup>L. N. Bulaevskii, A. I. Buzdin, M. L. Kuli, and S. V. Panjukov, *Adv. Phys.* **34**, 175 (1985).
- <sup>3</sup>K. P. Sinha and S. L. Kakani, *Magnetic Superconductors: Recent Developments* (Nova Science Publishers, New York, 1989).
- <sup>4</sup>O. Fischer, *Magnetic Superconductors* (Elsevier, Amsterdam, 1990), vol. 5.
- <sup>5</sup>M. B. Maple, *Physica B* **215**, 110 (1995).
- <sup>6</sup>M. L. Kulić, *C. R. Phys.* **7**, 4 (2006).
- <sup>7</sup>W. A. Fertig, D. C. Johnston, L. E. DeLong, R. W. McCallum, M. B. Maple, and B. T. Matthias, *Phys. Rev. Lett.* **38**, 987 (1977).
- <sup>8</sup>M. Ishikawa and O. Fischer, *Solid State Commun.* **23**, 37 (1977).
- <sup>9</sup>P. C. Canfield, S. L. Bud'ko, and B. K. Cho, *Physica C* **262**, 249 (1996).
- <sup>10</sup>S. S. Saxena *et al.*, *Nature (London)* **406**, 587 (2000).
- <sup>11</sup>D. Aoki, A. Huxley, E. Ressouche, D. Braithwaite, J. Flouquet, J.-P. Brison, E. Lhotel, and C. Paulsen, *Nature (London)* **413**, 613 (2001).
- <sup>12</sup>K. Machida and H. Nakanishi, *Phys. Rev. B* **30**, 122 (1984).
- <sup>13</sup>G. W. Crabtree, F. Behroozi, S. A. Campbell, and D. G. Hinks, *Phys. Rev. Lett.* **49**, 1342 (1982).
- <sup>14</sup>G. W. Crabtree, R. K. Kalia, D. G. Hinks, F. Behroozi, and M. Tachiki, *J. Magn. Magn. Mater.* **54-57**, 703 (1986).
- <sup>15</sup>D. E. Moncton, D. B. McWhan, P. H. Schmidt, G. Shirane, W. Thomlinson, M. B. Maple, H. B. MacKay, L. D. Woolf, Z. Fisk, and D. C. Johnston, *Phys. Rev. Lett.* **45**, 2060 (1980).
- <sup>16</sup>S. K. Sinha, G. W. Crabtree, D. G. Hinks, and H. Mook, *Phys. Rev. Lett.* **48**, 950 (1982).
- <sup>17</sup>E. I. Blount and C. M. Varma, *Phys. Rev. Lett.* **42**, 1079 (1979).
- <sup>18</sup>D. E. Moncton, D. B. McWhan, J. Eckert, G. Shirane, and W. Thomlinson, *Phys. Rev. Lett.* **39**, 1164 (1977).
- <sup>19</sup>J. M. DePuydt, E. D. Dahlberg, and D. G. Hinks, *Phys. Rev. Lett.* **56**, 165 (1986).
- <sup>20</sup>H. Matsumoto, H. Umezawa, and M. Tachiki, *Solid State Commun.* **31**, 157 (1979).
- <sup>21</sup>P. W. Anderson and H. Suhl, *Phys. Rev.* **116**, 898 (1959).
- <sup>22</sup>M. Tachiki, H. Matsumoto, and H. Umezawa, *Phys. Rev. B* **20**, 1915 (1979).
- <sup>23</sup>K. E. Gray, J. Zasadzinski, R. Vaglio, and D. Hinks, *Phys. Rev. B* **27**, 4161 (1983).
- <sup>24</sup>A. I. Buzdin, L. N. Bulaevskii, and S. V. Panyukov, *Zh. Eksp. Teor. Fiz.* **87**, 299 (1984).
- <sup>25</sup>A. I. Buzdin and A. S. Mel'nikov, *Phys. Rev. B* **67**, 020503(R) (2003).
- <sup>26</sup>S. Okada, K. Kudou, T. Shishido, Y. Satao, and T. Fukuda, *Jpn. J. Appl. Phys., Part 2* **35**, L790 (1996).
- <sup>27</sup>T. Shishido, J. Ye, T. Sasaki, R. Note, K. Obara, T. Takahashi, T. Matsumoto, and T. Fukuda, *J. Solid State Chem.* **133**, 82 (1997).
- <sup>28</sup>R. Prozorov, R. W. Giannetta, A. Carrington, and F. M. Araujo-Moreira, *Phys. Rev. B* **62**, 115 (2000).
- <sup>29</sup>R. Prozorov, R. W. Giannetta, A. Carrington, P. Fournier, R. L. Greene, P. Guptasarma, D. G. Hinks, and A. R. Banks, *Appl. Phys. Lett.* **77**, 4202 (2000).
- <sup>30</sup>R. Prozorov and R. W. Giannetta, *Semicond. Sci. Technol.* **19**, R41 (2006).
- <sup>31</sup>M. D. Vannette, A. Safa-Sefat, S. Jia, S. A. Law, G. Lapertot, S. L. Bud'ko, P. C. Canfield, J. Schmalian, and R. Prozorov, *J. Magn. Magn. Mater.* **320**, 354 (2008).
- <sup>32</sup>J. Feder, S. R. Kiser, and F. Rothwarf, *Phys. Rev. Lett.* **17**, 87 (1966).
- <sup>33</sup>R. Prozorov, *Phys. Rev. Lett.* **98**, 257001 (2007).